

# ELECTRONIC CONTROLLED BI-DIRECTIONAL CONTROLLER OF INDUCTION GENERATOR CONNECTED TO A SINGLE-PHASE GRID

Ricardo Quadros Machado, Enes Gonçalves Marra and José Antenor Pomilio

School of Electrical and Computer Engineering - FEEC

State University of Campinas - UNICAMP

Campinas - SP- 13081-970

BRAZIL

ricardom@dsce.fee.unicamp.br

**Abstract** - The cage-rotor three-phase induction generator (IG) presents considerable advantages mainly due to its robustness and low cost. However, the low performance in terms of voltage and frequency stabilization is an important drawback to guarantee the power quality. This paper contributes in presenting an IG-based structure which employs power-electronic converters associated with induction generator in order to improve both voltage and frequency stabilization. Moreover, the structure does not require the use of speed governor to the generator. This fact facilitates the application of the systems in micro-hydroelectric power plants in rural areas. The use of single-phase distribution lines to supply rural areas has been a common practice at utility companies. This study proposes some alternatives to connect three-phase inductor generator power plants to the single-phase grids. The grid can either supply additional electric power to AC local loads or absorb the exceeding generated power. The power electronic converters are controlled by a DSP that determines the power flow and the current waveforms at different points of the systems.

## I. INTRODUCTION

The attempt to use the Induction Generator (IG) as a cost-advantageous alternative has been the goal of several investigations [1-6]. The numerous well-known advantages of the three-phase induction machine has encouraged significant efforts in seeking suitable approaches able to overcome the IG poor voltage-regulation characteristics as well as synchronous-frequency variation. Some advantages of the induction-machines are its robustness, simple construction, little maintenance requirements, wide availability, low cost, and higher power-weight ratio (W/kg) than other kind of electrical machines.

In low population density rural areas, the electric power available may be single-phase. Customers in these areas may request three-phase electric power and find that it is uneconomical for the utility to meet the relatively low power needs [7]. On the other hand, there might be energy sources available to produce electric power. Considering this scenario, some authors have proposed the direct connection of the three-phase IG to single-phase utility grids, as a mechanism to obtain three-phase balanced voltages [8-11]. This connection is the so-called 'Steinmetz' connection, which has been used for three-phase motors [8]. However, these alternatives are able to operate only under strict circumstances and are disturbed by the AC load impedance variations. The purpose of this work is to present a feasible methodology to balance the

IG three-phase voltages and currents when the system is connected to a single-phase line.

## II. UNCOMPENSATED SYSTEM STRUCTURE

The direct connection of a three-phase IG to a single-phase utility grid as described in Fig. 1, causes strongly unbalanced line-voltages and line-currents at the generator terminals, as well as the presence of harmonic voltage and current distortions. The Fig. 2 presents the line voltages and the currents at the IG stator obtained through an experimental set-up of the system in Fig. 1. The single-phase RMS grid voltage is 220 V and the synchronous frequency is 60 Hz.

## III. PROPOSED-SYSTEM STRUCTURE

The proposed system comprises a IG connected to the single-phase utility grid by means of a Three-Phase static power-Converter (TPC) and a hysteresis-controlled Single-Phase power-Converter (SPC). In addition, a three-phase capacitor bank ( $C_{AC}$ ) is employed to provide the magnetization current to the IG.

Three-phase customer's loads are connected to the IG leads on the AC side of the system, as shown in Fig. 3. In circumstances of total customer's load absence all generated electrical power (losses neglected) is sent to the utility grid.

One feature of the proposed system is that it does not comprise any speed-governor for the IG, so the generated power depends on the prime-mover power availability. All the power-flux control is based upon the DC side voltage ( $V_{DC}$ ) control. Thus  $V_{DC}$  is the system control-variable, which is adjusted though setting a suitable value for the single-phase current ( $i_{sng}$ ). Therefore, the power-flow control is naturally achieved by the  $V_{DC}$  control [6]. As IG synchronous frequency and line voltages are kept constant by the TPC, the rotor-speed as well as the generator slip are completely determined by the association of the prime-mover with IG torque-speed characteristic curves [5].

On the one hand, when the generated power exceeds the AC customer's demand, the exceeding power is sent to the single-phase grid in co-generator operation mode. On the other hand, when the AC load power demand is higher than the electric power converted by the IG prime-mover system, the utility grid is able to supply the power deficit through the single-phase line/SPC/TPC structure.

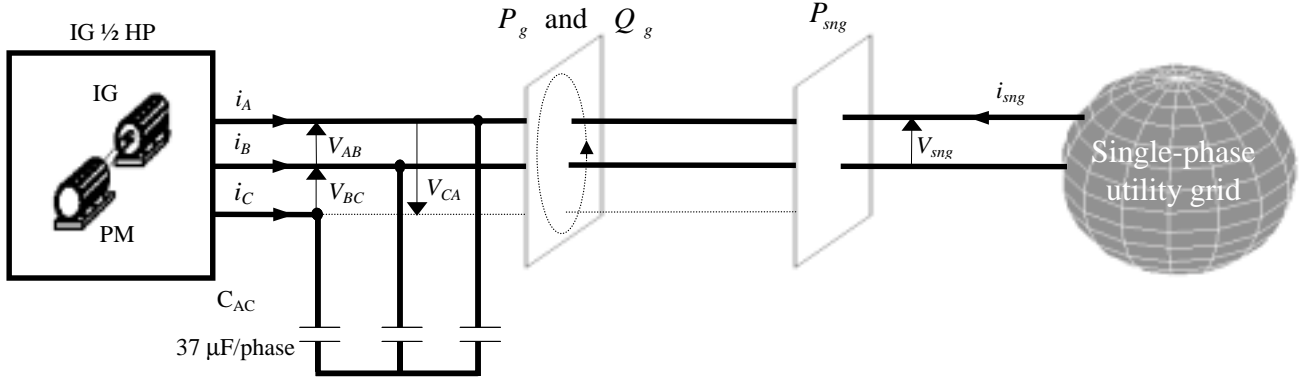
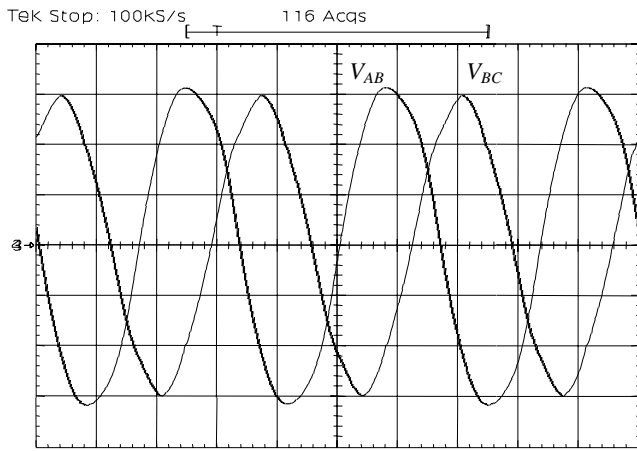
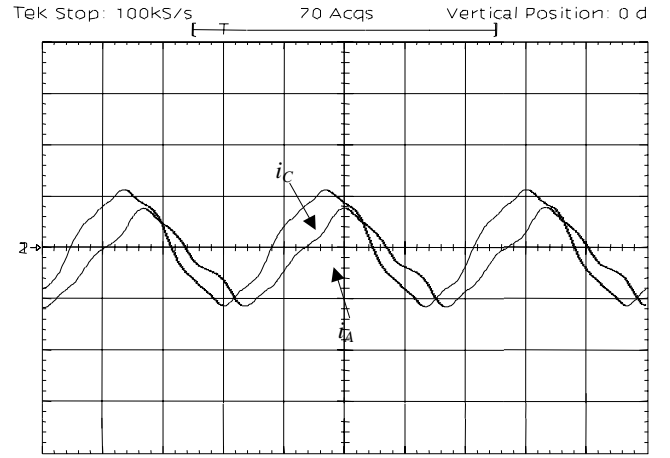


Fig. 1. IG directly connected to the single-phase utility grid.



IG line voltages.  
Vertical: Ch1 = Ch2 100 V/div., Horizontal: 5 ms/div.



IG line currents.  
Vertical: Ch1 = Ch2 2 A/div., Horizontal: 5 ms/div.

Fig. 2 - IG line-voltages and line-currents for the direct connection between IG and single-phase grid.

#### IV. CONTROL STRATEGY

The SPC and the TPC are connected between IG and single-phase utility grid. The SPC works using hysteresis current control. The current amplitude from the single-phase converter is defined by the DC link power balance, which affects the DC-link voltage. The SPC is connected to the single-phase grid through an inductor ( $L_{sng}$ ).

The DC-link voltage is compared with the DC voltage reference ( $V_{DCref}$ ), resulting in an error according to (1).

$$e = V_{DCref} - V_{DC} \quad (1)$$

The error is amplified and integrated as in (2), Where  $u_l$  is the proportional-integral controller (PI) output.

$$u_l = k_p \cdot e + k_i \cdot \int e \cdot dt \quad (2)$$

The current imposed by the SPC  $i_{sng}$  to the single-phase grid is defined by multiplying the control output voltage by the sample of the single-phase voltage waveform.

$$i_{sngref} = V_{sng} \cdot u_l \quad (3)$$

Where, the  $i_{saref}$  and  $i_{sbref}$  are the SPC reference in the each converter phase. These references are applied into the Hysteresis Current Control (HCC) modules.

$$i_{saref} = i_{sngref} \text{ and } i_{sbref} = -i_{sngref} \quad (4)$$

The TPC is a three-phase bi-directional converter, controlled by Space-Vector-Modulation (SV-PWM). The IG is connected to the AC side of the TPC side through a filter inductance ( $L_f$ ). The DC capacitor ( $C_{DC}$ ) is employed as the voltage source at the DC side of both TPC and SPC converters. The fundamental frequency and voltage at the TPC AC side is kept constant creating a constant frequency and voltage bus bar at the IG leads.

As the AC voltage is stabilized by the TPC, independently of the load, the system provides an automatic compensation of reactive loads, eliminating the problem associated with the inductive loads that, in other IG systems, usually demagnetize the generator.

#### V. SIMULATION RESULTS

##### A. Operation without Load

The association of the IG with the TPC and SPC converters (Fig. 3) produces a satisfactory compensation of the AC currents ( $i_A$ ,  $i_B$ ,  $i_C$ ), as well as produces balanced

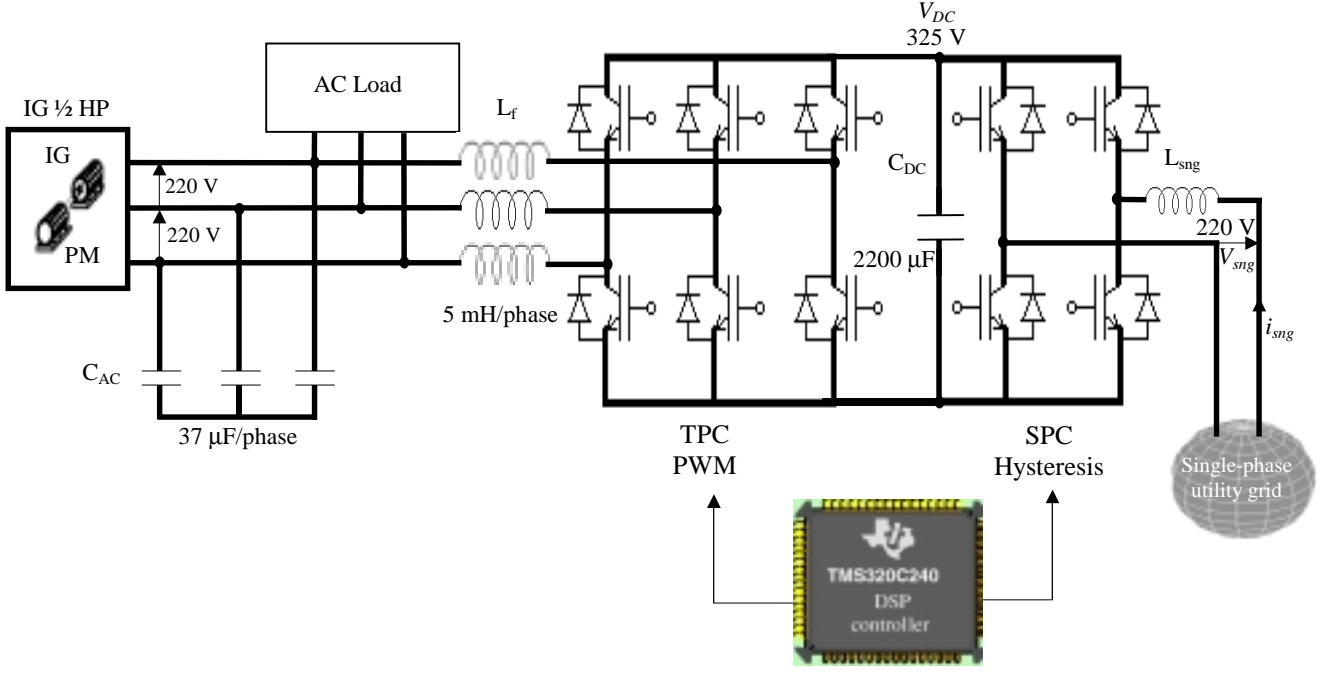


Fig. 3. General structure of the proposed system.

line voltages ( $V_{AB}$ ,  $V_{BC}$ ,  $V_{CA}$ ) at the IG leads. The Fig. 4 presents line-voltages (4.a) and line-currents (4.b) at the IG leads, and the DC link voltages ( $V_{DC}$ ), which is regulated by the control action (Fig. 4.c). The current sent to the single-phase grid by the SPC converter is controlled to have a sinusoidal waveform as shown in Fig. 4.d. The Figs. 4.e and 4.f present the average active and reactive power at the IG, at the static converter and at the single-phase grid. As there is no AC load, all the active power produced by the IG ( $P_g$ ) flows to the TPC and SPC converters ( $P_{con}$ ), so that  $P_g = P_{con}$ . Thus, the active power produced is sent to the single-phase grid ( $P_{sng}$ ) in order to maintain  $V_{DC}$  constant (Fig. 4.e), therefore  $P_g$ ,  $P_{con}$  and  $P_{sng}$  curves are superimposed to each other. Regarding the reactive power, Fig. 4.f depicts that the reactive power produced by the TPC and SPC converters ( $Q_{con}$ ) are exactly that one required by the IG- $C_{AC}$  capacitor set ( $Q_g$ ), as there is no AC load connected.

### B. Single-Phase Load Operation

In case, the three-phase load represented in Fig. 3 is substituted by a load connected between phases B and C, whose rated power is higher than the power produced by the IG, the power deficit is provided by the utility.

As shown in Fig. 5 both, IG line-voltage (Fig. 5.a) and line-currents (Fig. 5.b) are not anymore perfectly balanced due to the single-phase load, although the line-voltages are nearly balanced. At the instant when the single-phase is connected, the  $V_{DC}$  voltage presents a sag, which is corrected by the action of the PI DC-link voltage controller (Fig. 5.c).

When the single-phase load is connected, the single-phase current ( $i_{sng}$ ) presents an inversion of  $180^\circ$  (Fig. 5.d), as from this instant ahead the grid provides the power deficit required by load.

The Fig. 5.e shows the single-phase load current ( $i_L$ ), and Fig. 5.f describes the behavior of the average power of the IG ( $P_g$ ), the TPC and SPC converters power ( $P_{con}$ ), the single-phase grid power ( $P_{sng}$ ) and the single-phase load power ( $P_L$ ). The IG power remains the same ( $P_g$ ), once  $P_g$  is defined by the constant power of the prime mover. As a result, the power-flux in both TPC and SPC converters ( $P_{con}$ ) is inverted, so that the single-phase grid provides the power difference between the generated power and the load demanded. This test demonstrates that the IG-system is able to feed a load, whose power is greater than the generated power, obtaining part of the load demanded from single-phase utility grid.

The reactive power compensated by the TPC and SPC converters ( $Q_{con}$ ) now comprises the IG- $C_{AC}$  capacitor reactive demand ( $Q_g$ ) plus the oscillating reactive power of the single-phase load, as seen in Fig. 5.g.

### C. Three Phase Non-Linear Load Operation

Now, the three-phase non-linear load is connected (Fig. 3). However, the load consumption is about 73% of the generated power.

As shown in Fig. 6 both, IG line-voltage (Fig. 6.a) and line-currents (Fig. 6.b) are anymore perfectly sinusoidal when a non-linear load is present.

When the load is connected, the small sag is observed and corrected by the PI DC-link controller (Fig. 6.c).

The Fig. 6.e shows the three-phase load current ( $i_{LA}$ ,  $i_{LB}$  and  $i_{LC}$ ), and Fig. 6.f displays the behavior of the IG average power ( $P_g$ ), the TPC and SPC converters power ( $P_{con}$ ), the grid power ( $P_{sng}$ ) and the non-linear load power ( $P_L$ ). The IG power remains the same ( $P_g$ ), once it is given by the prime mover. As a result, the power-flux in both TPC and SPC converters ( $P_{con}$ ) is the difference between  $P_g$  and  $P_L$ .

The reactive power, Fig. 6.g depicts that the reactive power produced by the TPC and SPC converters ( $Q_{con}$ ) are exactly that one required by the IG- $C_{AC}$  capacitor set ( $Q_g$ ).

## VI. EXPERIMENTAL RESULTS

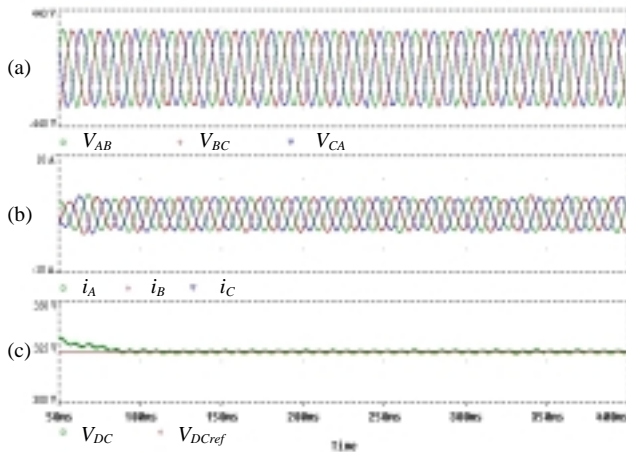
The DSP controller (20 MIPS, 16 bits and fixed point) TMS320F240 from Texas Instruments was employed to determine and to control the current to be injected into the single-phase utility grid, in order to archive power balance and DC side voltage control [12-14].

Experimental results were obtained from the implementation of the structure presented in Fig. 3 using the induction machine whose parameters are presented in table I. A commercially available IGBT based inverter was

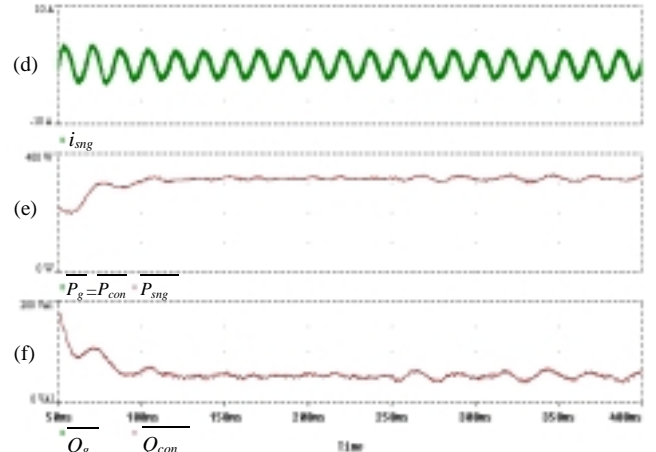
employed as the TPC. The values of the other components are:  $C_{AC} = 37\mu F$ ,  $C_{DC} = 1400\mu F$ ,  $L_f = 5mH$ .

Table I

Parameters of the induction machine at 60 Hz	
Stator resistance ( $r_s$ )	4.4 $\Omega$
Rotor resistance ( $r_r$ )	5.02 $\Omega$
Leakage stator inductance ( $X_s$ )	5.9 $\Omega$
Leakage rotor inductance ( $X_r$ )	5.9 $\Omega$
Linkage inductance ( $X_m$ ) ( $2 \cdot 60 \cdot L_{ms}$ )	70.53 $\Omega$
Iron and mechanical losses resistance ( $R_m$ )	582 $\Omega$
Rated power	1/2 hp
Number of poles (P)	4
Rotor inertia (J)	0.0006 kg.m <sup>2</sup>

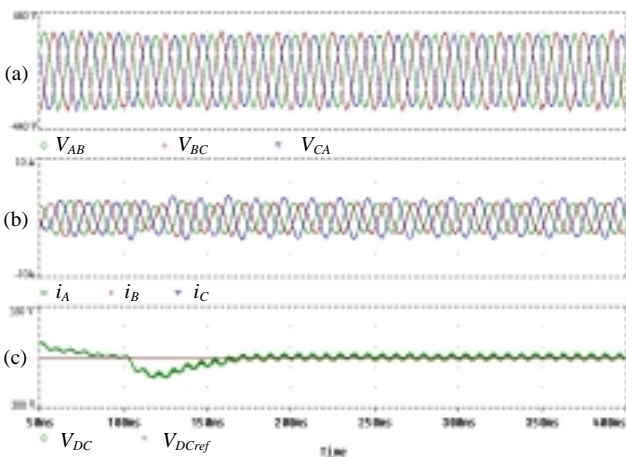


(a) IG line voltages.  
(b) IG line currents.  
(c) DC and reference voltages.

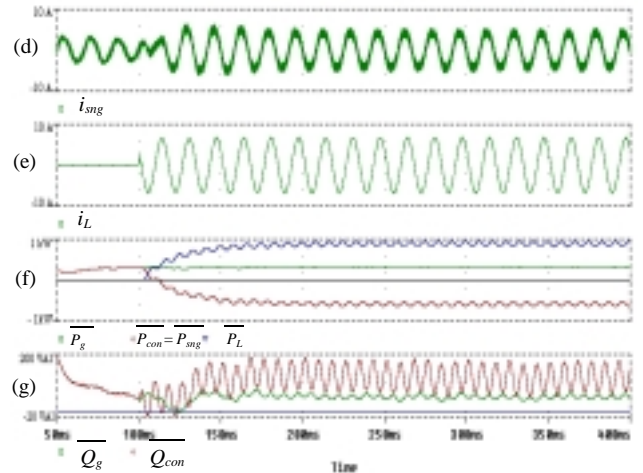


(d) Single-phase grid current.  
(e) Average active power in the IG, the converters and single-phase line.  
(f) Average reactive power in the IG and converters.

Fig. 4. Waveform when system operates without AC load.



(a) IG terminal voltages.  
(b) IG line currents.  
(c) DC and reference voltages.



(d) Single-phase grid current,  
(e) Load current.  
(f) Average active power in the IG, the converters, single-phase line and load.  
(g) Average reactive power in the IG and converters.

Fig. 5. Waveform when system operates with AC single-phase load.

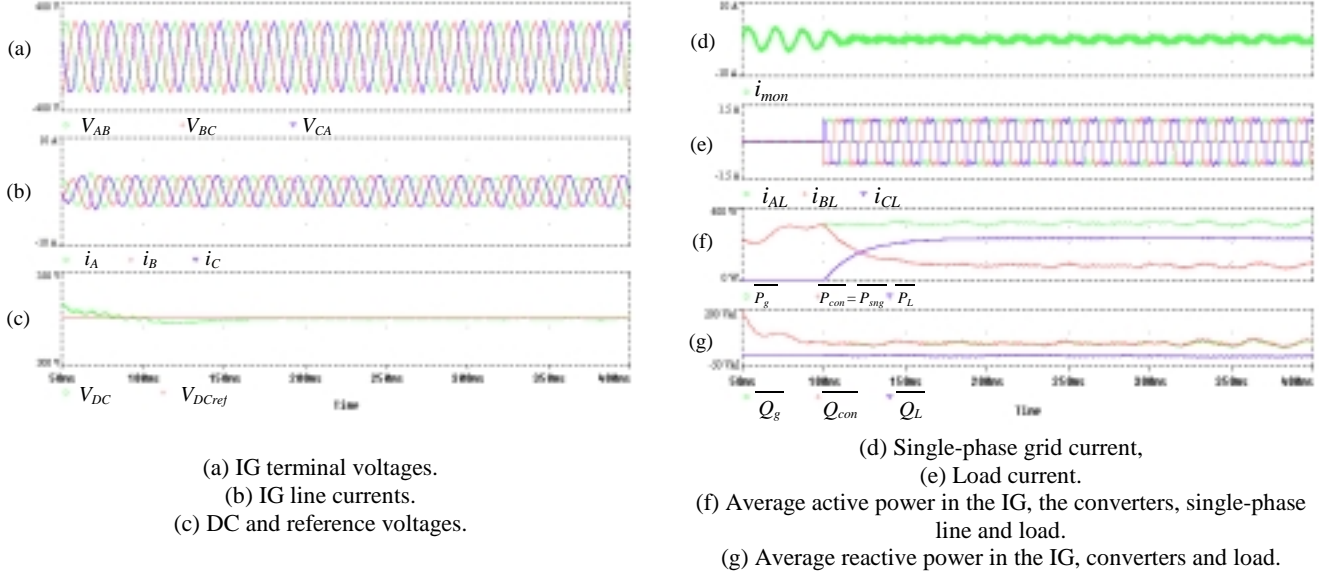


Fig. 6. Waveform when system operates with AC non-linear load.

#### A. Operation under Non-Load

Fig. 7.a presents the single-phase grid voltage ( $V_{sng}$ ) and the single-phase grid current ( $i_{sng}$ ), which is assumed to be positive when flowing from the grid to the IG-system. Notice that  $V_{sng}$  and  $i_{sng}$  are  $180^\circ$  displaced to each other, which means the power, is sent from the IG-system to the grid. The high-frequency components of the  $i_{sng}$  are due to the hysteresis current-control.

The Fig. 7.b presents the line currents at the IG leads in each one of its phases ( $i_A$ ,  $i_B$ ,  $i_C$ ). The currents are  $120^\circ$  displaced to each other and their magnitudes are slightly different due the induction-machine construction asymmetries.

#### B. Operation Under Non-Linear Three-Phase Load

A three-phase diode rectifier feeding a  $470 \mu\text{F}$  capacitor paralleled to a resistor was connected as load, whose rated power was about 110% of the power produced by the IG.

Fig. 8.a shows that the current  $i_{sng}$  remains sinusoidal in such a condition. Fig. 8.b shows that DC link voltage ( $V_{DC}$ ) is satisfactorily controlled even under non-linear load conditions.

### VII. CONCLUSIONS

This article presents the realization of a new strategy to compensate for unbalanced operation of an induction generator when connected to a single-phase grid. In the proposed system, a three-phase static power converter was employed to guarantee three-phase fixed frequency to the IG. Every sort of power difference between the IG generated power and the AC load demand reflects in the DC-link voltage, so that  $V_{DC}$  is used to control the system power balance. When the generated power is greater than the consumed power, the single-phase power converter

sends the exceeding power to the single-phase utility grid, avoiding the increment of  $V_{DC}$ . On the contrary, when the consumed power is greater than the IG generated power, the SPC converter absorbs power from the grid, in order to supply the power deficit required by AC load. In both modes of operation (sending or absorbing power from the utility grid), the SPC converter assures the grid current attains good quality, through a DSP hysteresis current control. The system proved to work properly even under unbalanced AC-load or under non-linear load circumstances.

### VIII. ACKNOWLEDGMENT

The authors would like to acknowledge CAPES and FAPESP (proc. 98/11170-2 and 00/11038-9) for supporting this project, and Texas Instruments for the DSP donation.

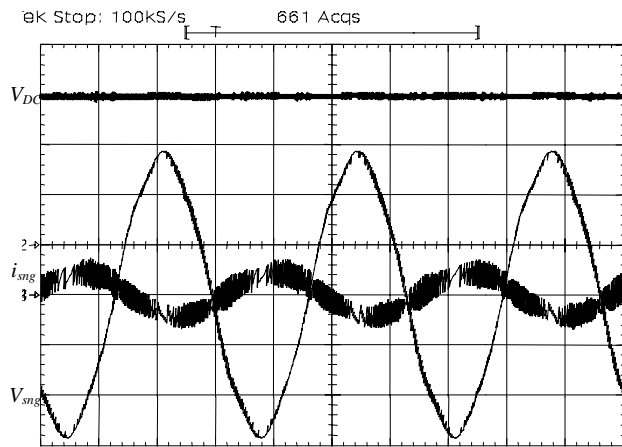
### IX. REFERENCES

- [1] D. E. Basset and M. F. Potter, "Capacitive excitation for induction generator," *AIEE Transactions*, vol. 54, pp. 540-543, 1935.
- [2] C. F. Wagner, "Self-excitation of induction motors," *AIEE Transactions*, vol. 58, pp. 47-51, 1939.
- [3] E. H. Watanabe and A. N. Barreto, "Self-excitation of induction generator force-commutated rectifier system operating as a DC power supply," *IEE Proceedings*, vol. 134, Pt. B, no. 5, pp. 255-260, 1987.
- [4] L. Wang and S. Jina-Yi, "Effects of long-shunt and short-shut on voltage variations of self-excited induction generator," *IEEE Trans. on Energy Conversion*, vol. 12, no. 4, pp.368-374, 1997.
- [5] E. G. Marra and J. A. Pomilio, "Self-excited induction generator controlled by a VS-PWM bi-directional converter for rural applications," *IEEE Trans. on Industrial Applications*, vol. 35, no. 4, pp. 877-883, 1999.
- [6] E. G. Marra and J. A. Pomilio, "Induction generator based system providing regulated voltage with constant frequency," *IEEE Trans. on Industrial Electronics*, vol. 47, no. 4, pp. 908-914, 2000.

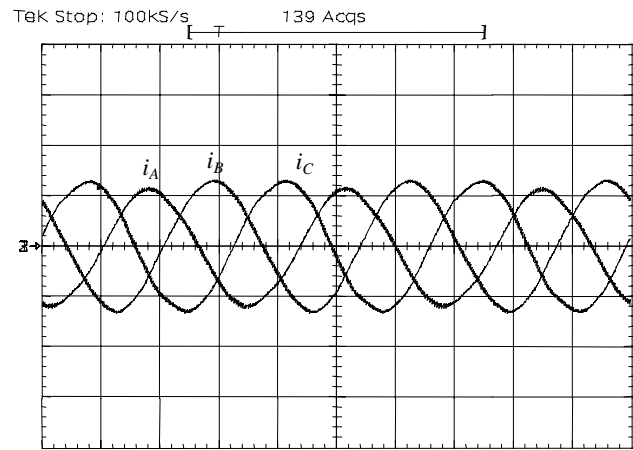


- [7] W. A. Moncrief, "Practical application and selection of single-phase to three-phase converters," *Proceedings of IEEE/IAS Rural Electric Power Conference*, pp. D3-1/D3-9, 1996.
- [8] T. F. Chan, "Effect of rotational direction on the performance of a three-phase induction generator connected to the single-phase power system," *Proceedings of IEMDC*, Milwaukee, USA, pp. MB1-6.1-MB1-6.3, 1997.
- [9] J. L. Bhattacharya and J. L. Woodward, "Excitation balancing of a self-excited induction generator for maximum power output," *IEE Proceedings*, vol. 135, Pt. C, no. 2, pp. 88-97, 1998.
- [10] J. M. O. Durham and R. Ramakumar, "Power system balancers for an induction generator," *IEEE Trans. on Industrial Applications*, Vol. IA-23, no. 6, pp. 1067-1072, 1997.

- [11] O. J. Smith, "Three-phase induction generator for single phase line," *IEEE Trans. on Energy Conversion*, Vol. 2, no. 3, 1987.
- [12] I. Panahi, M. S. Arefeen and Z. YU, "DSP excel in motor-control applications," *Edn Magazine*, pp. 111-118, 1997.
- [13] M. S. Arefeen, D. Figoli and Z. Yu, "Integrating multiple motor control functions using a single DSP controller," *Proceedings of APEC*, Dallas, USA, pp. 813-8118, 1999.
- [14] W. Shireen, M. S. Arefeen and D. Figoli, "Controlling multiple motors utilizing a single DSP controller," *Proceedings of APEC*, Dallas, USA, pp. 807-812, 1999.

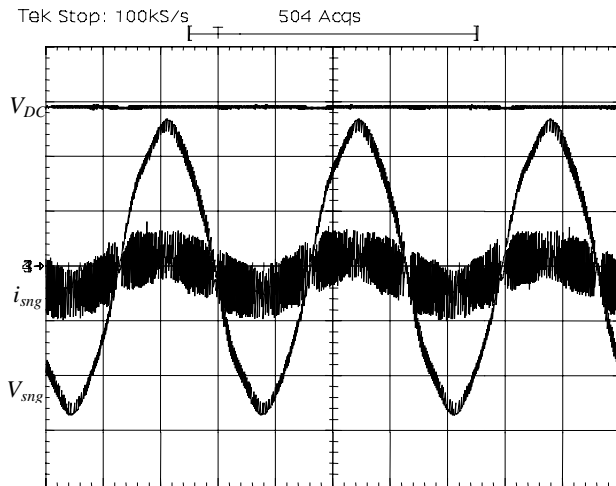


(a) DC voltage ( $V_{DC}$ ), voltage ( $V_{sng}$ ) and current ( $i_{sng}$ ) in single-phase grid.  
Vertical: Ch2 100 V/div.; Ch3 2 A/div.; Ch4 100 V/div.  
Horizontal: 5 ms/div.

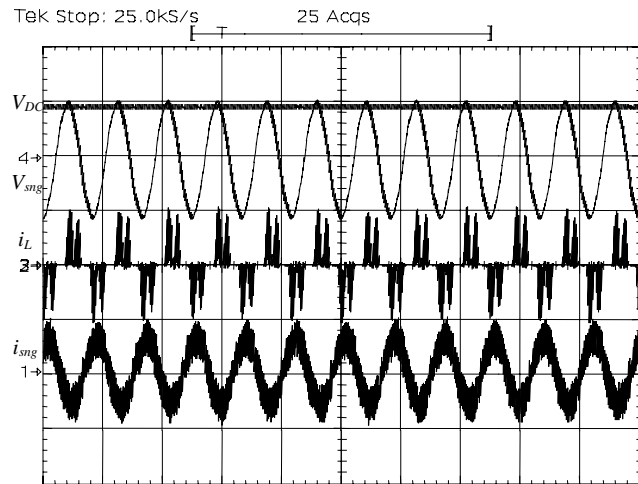


(b) Line currents from IG.  
Vertical: Ch2 = Ch3 = Ch4 2 A/div.  
Horizontal: 5 ms/div.

Fig. 7. Experimental results with no-load operation.



(a) DC voltage ( $V_{DC}$ ), voltage ( $V_{sng}$ ) and current ( $i_{sng}$ ) in the single-phase grid.  
Vertical: Ch1 1 A/div.; Ch3 100 V/div.; Ch4 100 V/div.  
Horizontal: 5 ms/div.



(b) DC voltage ( $V_{DC}$ ), voltage ( $V_{sng}$ ), current ( $i_{sng}$ ) in the single-phase grid and AC load line current ( $i_L$ ).  
Vertical: Ch1=Ch2 1 A/div.; Ch3 100 V/div.; Ch4 250 V/div.  
Horizontal: 20 ms/div.

Fig. 8. Experimental results with non-linear three-phase load.